Eur Biophys J (1986) 13:235–243

European Biophysics Journal

Computer reconstruction of the spread of excitation in nerve terminals with inhomogeneous channel distribution

A. Peres and F. Andrietti

Dipartimento di Fisiologia e Biochimica generali, Laboratorio di Elettrofisiologia dell'Università di Milano
Via Celoria, 26, I-20133 Milano, Italy

Received May 7, 1985/ Accepted in revised form October 14, 1985

Abstract. A direct numerical integration method, as modified by Du Fort and Frankel (1953), has been used to solve the partial differential equation system which describes the spread of action potential in a mammalian nerve terminal. Branching of the terminal as well as inhomogeneous distributions of Na^+ and K^+ voltage-dependent channels (Brigant and Mallart 1982) have been incorporated in the model.

Using the channel densities and the kinetic parameters measured in the node of Ranvier, the depolarization in the terminal branches has an amplitude of only 60% of the action potential in the node. Furthermore, the time courses of the calculated membrane currents differ considerably from the ones measured by Brigant and Mallart (1982) and by Konishi and Sears (1984).

Increasing the Na^+ and K^+ channel densities may considerably increase the terminal depolarization and also reproduce qualitatively the current waveforms observed experimentally. The model can also reproduce some of the effects of pharmacological channel blocks.

The simulation allows a new interpretation of the different components of membrane current along the terminal.

Key words: Nerve endings, action potential, computer simulation, membrane heterogeneity

Introduction

Neurotransmitter release is thought to be mediated by a voltage-dependent influx of Ca^{2+} in the motor nerve terminal. The problem of the active invasion of the terminals by the action potential is difficult to solve experimentally in vertebrate nerve endings because of the extremely small size of the preparation, which prevents the use of intracellular microelectrodes. Using less direct techniques, Katz and Miledi (1965) have been able to show active spread in frog presynaptic terminals. However, the situation in mammals appears to be different. Brigant and Mallart (1982) and Konishi and Sears (1984), measuring membrane currents with focal extracellular electrodes, have shown that different current waveforms are observed at different locations along the terminals: only inward current at the transition between the myelinated and non-myelinated parts of the axon, only outward current in the terminal branches and a triphasic wave in an intermediate zone. These observations, together with results obtained using specific channel blockers, lead Brigant and Mallart (1982) to conclude that, in mouse motor endings, Na^+ channels are present only in a narrow pre-terminal zone, the terminal branches being populated only by K^+ and Ca^{2+} channels. According to Konishi and Sears (1984), however, some inward Na^+ current is present even in the terminal zone.

A mathematical reconstruction of the spread of excitation from a myelinated axon to an unmyelinated terminal was performed by Khodorov and Timin (1975). However, in those calculations the membrane properties of the terminal were assumed to be identical to the ones of the myelinated part. Data on the kinetic properties of voltage-dependent Na^+ and K^+ channels in mammalian nodal and peri-nodal areas are now available (Chiu et al. 1979; Chiu and Ritchie 1981). Therefore, we thought it worthwhile, to try a numerical reconstruction of the action potential spread in mammalian motor endings using the published data on channel kinetics together with the proposed spatial membrane heterogeneity.

Electrical model and computation method

Geometry and channel distribution

Figure 1 illustrates the geometry of the model used in this work and the distribution of voltage-depen-

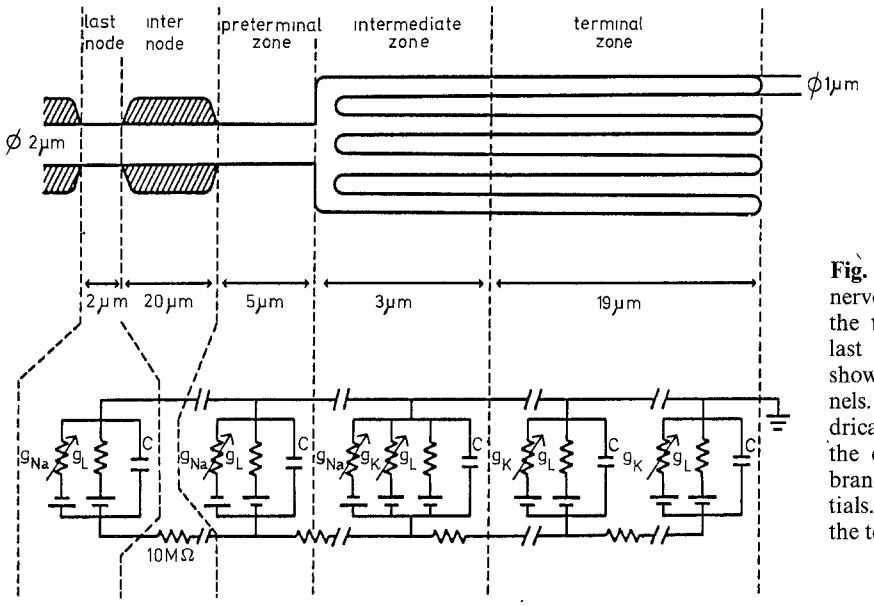

Fig. 1. Geometrical and electrical scheme of a nerve terminal used in this work. Excitation of the terminal was induced by stimulating the last node of Ranvier. The electrical model shows the non-uniform distribution of channels. Each circuit represents a 1 μm long cylindrical segment except for the last node where the circuit represents the whole nodal membrane. Batteries represent equilibrium potentials. Branching was included as explained in the text

dent channels. Excitation was induced by stimulating the last node of Ranvier, which was assumed to be 1 μm in radius and 2 μm long. This produced a longitudinal current in the last internode (20 μm long, Quick et al. 1979) which depolarized the preterminal zone. The geometry and the channel distribution were chosen on the basis of the morphological and electrophysiological observations of Brigant and Mallart (1982). The whole ending was divided in three longitudinal zones: *(1)* a pre-terminal zone, 1 μm in radius and 5 μm long, possessing only Na^+ and leakage channels; *(2)* an intermediate zone (3 μm long) where a ramification in four branches (0.5 μm in radius) occurs; this zone possesses Na^+, K^+ and leakage channels: the densities of Na^+ and K^+ channels respectively decrease and increase linearly with length, while the density of leakage channels remains constant; *(3)* a terminal zone (19 μm long) composed of the four branches where only K^+ and leakage channels are present.

Equations and parameters

$V(x,t)$ was obtained by integrating the partial differential equation:

$$\frac{1}{r_1}\frac{\partial^2 V}{\partial x^2} = c_m \frac{\partial V}{\partial t} + \sum_i i_i \qquad (1)$$

in which r_1 is the cytoplasmic resistance per unit length (Ohm/cm), c_m is the capacitance per unit length (F/cm) and i_i are the membrane ionic currents per unit length (A/cm). The ionic currents were described according to the usual Hodgkin-Huxley kind of model. Thus:

$$i_i = g_{Na}(V - V_{Na}) + g_K(V - V_K) + g_L(V - V_L), \qquad (2)$$

where V_{Na}, V_K and V_L are the zero-current potentials for sodium, potassium and leakage. The voltage- and time-dependent conductances were expressed as (Chiu et al. 1979; Chiu and Ritchie 1981):

$$\begin{aligned} g_{Na} &= \bar{g}_{Na} m^2 h \\ g_K &= \bar{g}_K n^4 \end{aligned} \qquad (3)$$

in which $\bar{g}_{Na}$ and $\bar{g}_K$ are the limiting conductances and m, h and n obey first-order equations of the kind:

$$\dot{y} = \alpha_y(1-y) - \beta_y y \qquad (4)$$

with the following equations for the rate constants:

$$\begin{aligned} \alpha_m &= \frac{0.029\,V + 10.1}{1 + \exp(-0.19\,(V+49))} \\ m_\infty &= \frac{1}{1 + \exp(-(V+55.6)/4.15)} \\ \beta_h &= \frac{1.25}{1 + \exp(-0.1\,(V+56))} \\ h_\infty &= \frac{1}{1 + \exp((V+74.4)/5.7)} \\ \alpha_n &= \frac{0.34\,((V+15)/15.9)}{1 - \exp(-(V+15)/15.9)} + 0.1 \\ \beta_n &= \frac{0.085\,((V+37.5)/12.2)}{\exp((V+37.5)/12.2) - 1}. \end{aligned} \qquad (5)$$

Equations for α_m and β_h are from Chiu et al. (1979); equations for m_∞ and h_∞ have been fitted to Fig. 7 of Chiu et al. (1979) and are for a rabbit node of Ranvier at 14 °C; equations for α_n and β_n are taken from Hille (1971) and are for a frog node at 22 °C. Although the rate constants for K^+ are from a dif-

Table 1. Standard parameters

Parameter	Symbol	Value	Units	Source
Limiting Na conductance	$\bar{g}_{Na}$	$0.11 \cdot 10^{-6}$	S	(1)
Limiting K conductance	$\bar{g}_K$	$0.034 \cdot 10^{-6}$	S	(2)
Leakage conductance	g_L	$0.011 \cdot 10^{-6}$	S	(1)
Internal resistance	R_i	171	Ohm · cm	(1)
Capacity	C	$0.002 \cdot 10^{-9}$	F	(1)
Na^+ 0-current potential	V_{Na}	51	mV	(1)
K^+ 0-current potential	V_K	−80	mV	(3)[a]
Leak 0-current potential	V_L	−80	mV	(1)

Sources: (1): Chiu et al. (1979)
(2): Chiu and Ritchie (1981)
(3): Hille (1971)

[a] The value given by Hille is in effect −75 mV. We used −80 mV to obtain a resting potential of −80 mV for the mammalian nerve.

ferent species, they appear to match reasonably the paranodal K^+ currents, provided they are multiplied by 1.6 (Chiu and Ritchie 1981). Since our purpose was to compare the calculations to the data of Brigant and Mallart, which were obtained at 22 °C, we multiplied all rate constants by 1.6 (Chiu et al. 1979; Chiu and Ritchie 1981).

The values of limiting conductances, leakage conductance, internal resistivity, membrane capacity and zero current potentials are listed in Table 1 and refer to a typical node of a mammalian myelinated nerve 5 μm in radius, 2 μm long (Chiu and Ritchie 1981; Chiu et al. 1979). These will be called the "standard parameters" in the following. The actual values used in the calculations will be derived from the standard parameters by appropriate scaling according to the geometry of the particular zone of the terminal.

Branching

The problem of impulse propagation in a branching axon has been treated by various authors (see for instance Khodorov and Timin 1975; Parnas and Segev 1979). These studies were generally concerned with factors affecting conduction block and did not include channel inhomogeneity. We introduced branching in our model in the following way. Since the four branches are identical and their radius is half the radius of the pre-terminal zone, they will behave electrically as a single cylinder having a cross section equal to that of the pre-terminal zone but with a surface area (per unit length) twice that of the preterminal zone. Therefore, the internal resistance per unit length will not change at the branching point, while all other parameters depending on surface area will double (per unit length) beyond the branching point. The whole terminal was therefore treated as a single cylinder with the appropriate changes in the parameters.

Calcium current

A complete description of the electrical events in a presynaptic terminal should include a voltage-dependent Ca^{2+} current. A kinetic description of the Ca^{2+} current in a nerve terminal is available only for the squid giant synapse (Llinas et al. 1981 a, b). However, simple calculations show that the Ca^{2+} current needed to raise the intracellular Ca^{2+} concentration to 1 mM (which should be well above the threshold level for vesicle fusion) over a period of 2 ms in a 1 μm long segment of a mammalian nerve ending is about 30 pA. This value is about 30-fold lower than the other ionic currents. Furthermore, an intracellular calcium elevation is likely to be important only in a shallow sub-membrane layer and to obtain this an even smaller Ca^{2+} current will be sufficient. Since the expected effects of this current appear to be small, and to avoid the heavy computing complications arising from the introduction of the complex kinetic equations proposed by Llinas et al. (1981 a), we decided to neglect this component in the mathematical model.

Computing method

Implicit methods of integration of Eq. (1) have been shown to be far superior to explicit ones (Moore et al. 1975). The reason for this lies in the fact that in order to have stability for an explicit method of integration of a parabolic differential equation the following inequality must hold (see, for example, Fox 1962, p. 246):

$$k/h^2 < 1/(2 c_m r_1) \tag{6}$$

between the step of time, k, and the step of space, h. On the other hand, implicit methods of integration are intrinsically stable and subject only to the limitations due to truncation errors. The difference between the two methods becomes more important when the value of h decreases; in this situation, k should decrease as h^2 in order to maintain inequality of Eq. (6).

For large cables a value of $h = 500$ μm is sufficiently small (Moore et al. 1975). In this case, the ratio between the computation time of the two different methods is 1:10 (Moore et al. 1975). In our case a much smaller value of h (1 μm) is necessary in order to have a good description of a system in which the length of the intermediate zone is only 3 μm. In this case application of (6) gives $k = 0.1$ μs, so that at least 30,000 complete iterations should be necessary to span 3 ms of the time axis.

On the other hand, the use of an implicit method requires a greater computational effort, necessary to solve the system of linear equations obtained from the implicit formula of the finite difference approximation.

A third way is to use a method which has unrestricted stability, while preserving the numerical advantages of explicit methods. This is what has been done in the present work by using the explicit formula given by Du Fort and Frankel (1953). In this way a satisfactory result has been obtained with $k = 2\,\mu s$, i.e. a value at least 20 times larger than that required by the normal explicit method. Since, in order to apply the method, we must know a second line of values in addition to the initial ones, a special starting procedure is necessary. So we have begun our integration with a normal explicit method, by letting $k = 0.04\,\mu s$, and we have shifted to the Du Fort and Frankel method after $2\,\mu s$. After this time the computation was continued with $k = 2\,\mu s$.

Due to the short internodal length near the terminal, several nodes may supply current to the terminal. However the presence of inward currents at the preterminal and intermediate zones indicates that the depolarization of the terminal depends on local excitation properties more than on passive spread. Under these conditions, the intensity of the stimulating current is not critical. Therefore the value of $\partial V/\partial x$ at the beginning of the nerve terminal was obtained by calculating the longitudinal current generated by a non-propagated action potential at the last node only, along the last internode resistance of 10^7 Ohm. The second boundary condition is given by $\partial V/\partial x = 0$ at the terminated end of the terminal.

The computation time required by a personal computer (M20 OLIVETTI), in interpreted BASIC language, for a single calculation between 0 and 2.9 ms, was about 2 h.

Results

Calculation with standard parameters

Figure 2 shows the results of the integration using standard parameters. In A, the time course of membrane potential at the middle of the three heterogeneous zones is shown. The action potential at the last node is also shown for comparison. The peak depolarization in the middle of the terminal zone reaches only -18 mV. In B, the total membrane current $(I_c + I_{Na} + I_K + I_L)$ at the same locations are shown. These three waveforms should be compared with the experimental observations of Brigant and Mallart (1982). It is clear that there is not good agreement, especially for the absence, in the computed traces, of double peaks in the pre-terminal and terminal zones. Also, the late outward current in the triphasic wave of the intermediate zone is very small compared to that observed experimentally.

It is clear that some changes in the parameters have to be made in order to attempt to simulate the experimental observations.

An increase in $\bar{g}_{Na}$ and $\bar{g}_K$ relative to g_L can simulate the experimental results

Since there are several parameters that can be changed it is very important to keep to a minimum number of changes and also to perform changes

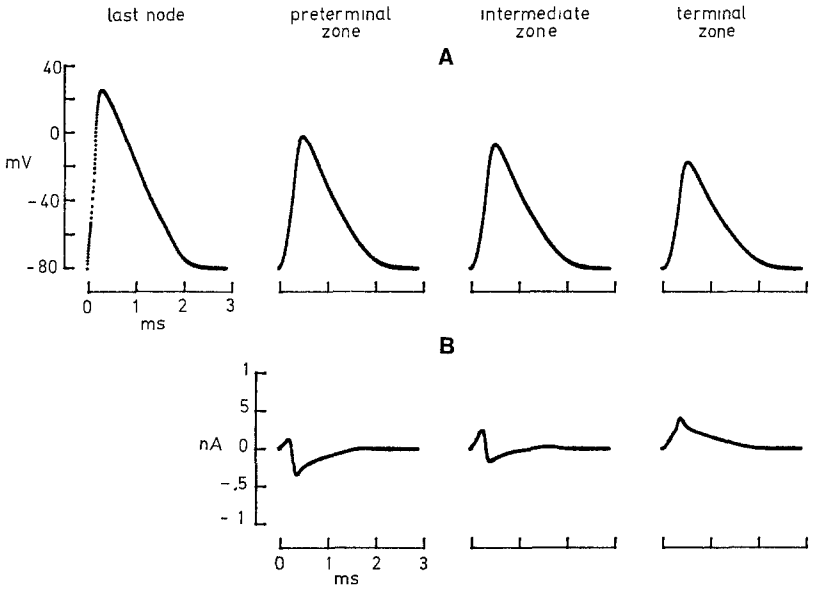

Fig. 2. **A** Action potentials in the node and in the middle of the three inhomogeneous zones computed using standard parameters (Table 2, column 3). **B** Total membrane currents in the corresponding zones

which are compatible with the physiological situation. We decided, rather arbitrarily, to avoid changes in the rate constants and to operate only on limiting conductances.

Furthermore, the results obtained with the standard parameters may indicate which change of parameters will be likely to be effective. The limited amplitude of the terminal depolarization can be attributed to the combined effect of the absence of Na^+ channels in the terminal parts and of the branching, which acts by reducing the effective space constant of the termination. A larger terminal depolarization may be produced by a stronger current from the parent axon. However, this will generate large outward currents (leakage and capacitive) in the preterminal zone, which were not observed experimentally. Alternatively, a larger depolarization may be obtained by increasing the Na^+ conductance in the preterminal zone or by allowing the presence of Na^+ channels even in the terminal branches (Konishi and Sears 1984).

A digression is needed at this point on the direction of the various components of the current and on their effect on the total membrane current. When the membrane potential is limited to the range -80 to $+50$ mV, the direction of the ionic currents is determined: Na^+ current could only be inward, K^+ and leakage currents could only be outward; however, the capacitive current could be either inward or outward depending on the sign of dV/dt. The interpretation given by Brigant and Mallart (1982) to explain the presence of a double peak of inward current in the pre-terminal zone is not satisfactory in this respect. In fact they propose that the second inward peak is not carried by Na^+ ions, but that it is due to a "sink" of the local circuit current produced by K^+ ions leaving the axoplasm at the terminal zone. However, according to what we have said above, in the pre-terminal zone the only ionic current which can flow inwardly is a Na^+ current, the other possible inward current being the capacitive current. An inward capacitive current, however, cannot be expected to be as large as the second inward peak observed experimentally, since this would imply an extremely fast repolarization. The conclusion is that we may suspect that the second inward peak at the pre-terminal zone might be carried again by Na^+ ions.

In effect, such a waveform is expected from the Hodgkin-Huxley formulation and arises when the inactivation of the Na^+ channels is slow compared to the K^+-induced repolarization of the action potential (Khodorov and Timin 1975; Chiu et al. 1979): in such circumstances the sodium current is dominated by its electrochemical gradient changes rather than by the conductance changes. An important condition required to obtain a double-peaked Na^+ current is that the membrane potential must approach V_{Na} rather closely. Therefore we might expect that the Na^+ conductance increase, needed to enhance the terminal depolarization, may also have the effect of producing a late inward peak in the pre-terminal current waveform. Another condition required to produce a second peak of inward Na^+ current is that the action potential has to repolarize faster than the development of Na^+ channel inactivation. In our case there are no K^+ channels in the pre-terminal zone, therefore the K^+ current in the intermediate and terminal zone must be large enough to produce significant effects on the pre-terminal zone. A high K^+ conductance may significantly reduce the terminal depolarization and so we decided, following

Table 2. Parameters used in the various calculations (all values are in μs)

1 Zone	2 Parameter	3 Standard value (Fig. 2)	4 Modified value (Fig. 3)	5 TEA value (Fig. 5)	6 TTX value (Fig. 7)
Pre-terminal	$\bar{g}_{Na}$	0.11	0.495	0.495	0
Intermediate	$\bar{g}_{Na}$	0.11 – 0	0.151 – 0.014	0.151 – 0.014	0.151 – 0.014 [a]
Terminal	$\bar{g}_{Na}$	0	0.014	0.014	0.014
Pre-terminal	$\bar{g}_K$	0	0	0	0
Intermediate	$\bar{g}_K$	0 – 0.034	0 – 0.68	0	0 – 0.68 [b]
Terminal	$\bar{g}_K$	0.034	0.68	0	0.68
Pre-terminal	g_L	0.011	0.011	0.011	0.011
Intermediate	g_L	0.011	0.0011	0.0011	0.0011
Terminal	g_L	0.011	0.0011	0.0011	0.0011

As in Table 1 all values are referred to the reference node 5 μm in radius, 2 μm long.
[a] Decreasing linearly with distance between the indicated values
[b] Increasing linearly with distance between the indicated values

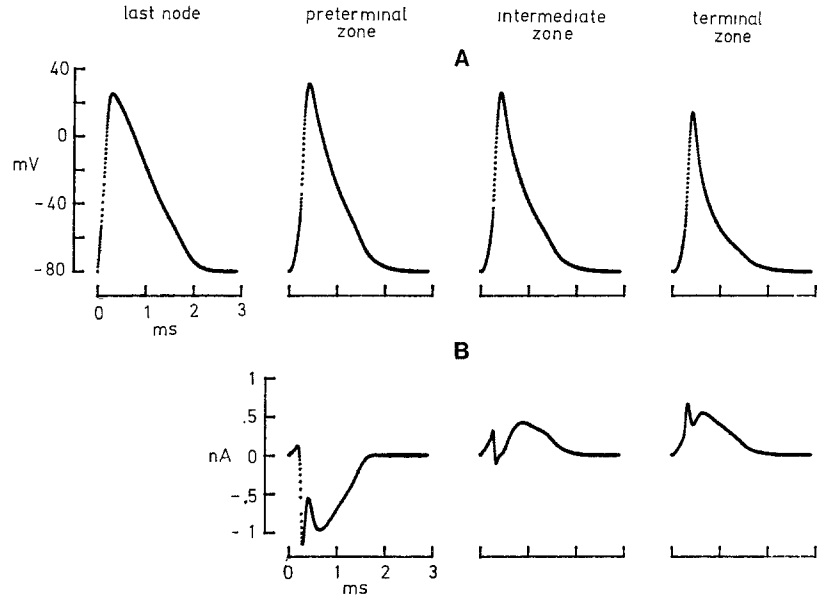

Fig. 3. Computation of action potentials and membrane currents using parameters modified in order to reproduce the experimental observations (Table 2, column 4). The appearance of double peaks in the pre-terminal and terminal zones and of a triphasic wave in the intermediate zone is accompanied by a larger depolarization of the membrane in all zones

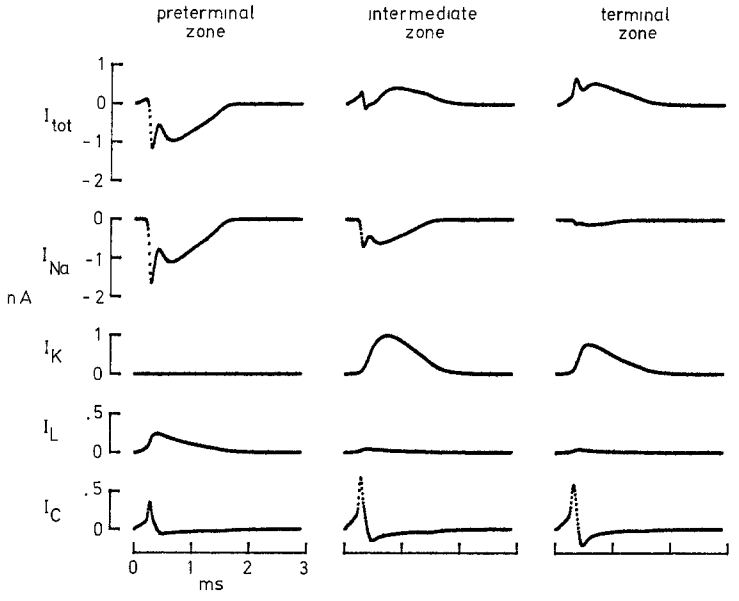

Fig. 4. Different components of membrane currents in the three zones (same parameters as in Fig. 3). The double inward peak in the pre-terminal zone is due mainly to the double peak of the Na^+ current, while the double outward peak in the terminal zone is due to both capacitive and K^+ currents. The triphasic wave in the intermediate zone arises from the contribution of all components

the suggestion of Konishi and Sears (1984), to introduce a small density of Na^+ channels in the terminal zone.

We then performed many calculations changing the standard parameters along the guidelines outlined above. Figure 3 shows the results of a computation in which the parameters were changed according to Table 2.

The current waveforms of Fig. 3 compare favourably (at least qualitatively) with the experimental ones (Brigant and Mallart 1982; Konishi and Sears 1984): double peaks are present in the pre-terminal and terminal waveforms and a triphasic wave appears in the intermediate zone. The various components of the total membrane current in the three zones are shown in Fig. 4 (same parameters as in Fig. 3). It can be seen that the double inward peak of the total current in the pre-terminal zone reflects the double peak of the Na^+ current, while the double outward peak in the terminal zone is due essentially to the capacitive current plus the K^+ current, while the intermediate triphasic wave is due to capacitive, Na^+ and K^+ currents.

Simulation of pharmacological block of the K^+ *current*

In order to identify the origin of the different components of their current waveforms, Brigant and Mallart (1982) applied selective blocking agents to their preparations, either dissolving them in the

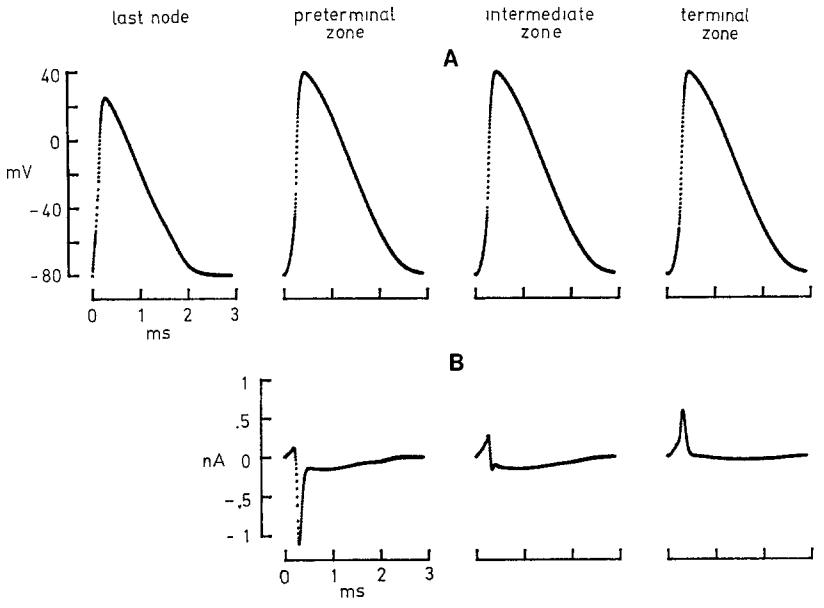

Fig. 5. Simulation of pharmacological block of K^+ channels. Setting the potassium conductance to zero everywhere (Table 2, column 5) causes an increase in amplitude and duration of the depolarization in all three zones. According to the experimental observations, the corresponding membrane currents in the pre-terminal and terminal zones lack the double peak and the one in the intermediate zone is no longer triphasic

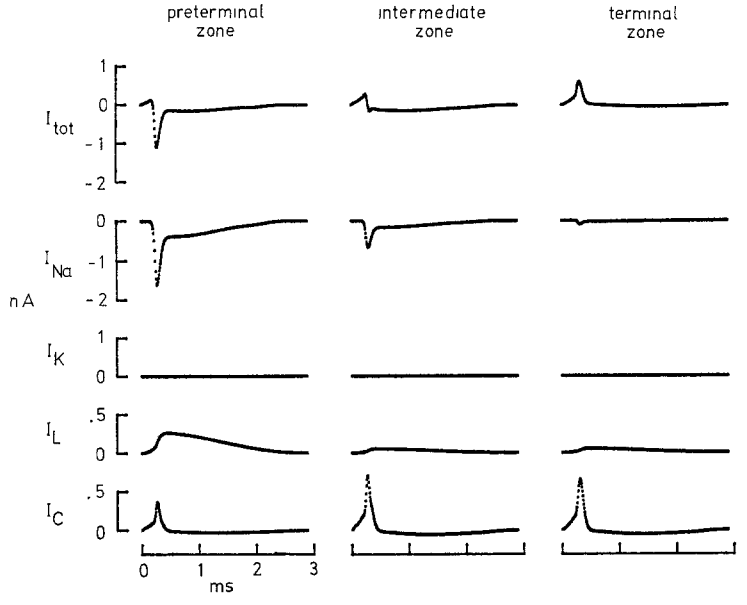

Fig. 6. Current components relative to Fig. 5. showing that the absence of double peaks is due to the absence of a double peak of the Na^+ current in the pre-terminal zone and to the absence of K^+ current in the terminal zone

bath or by local ionophoretic application. We have tried to reproduce these different experimental conditions in our simulations.

Application of K^+ channels blockers such as tetraethylammonium, 4-aminopyridine or 3,4-diaminopyridine in the bath eliminated the late peaks in the pre-terminal and terminal waveforms and changed the intermediate one from triphasic to biphasic. This experiment can easily be simulated simply by setting $\bar{g}_K = 0$ everywhere. Results of the calculation with the parameters of Table 2 (column 5) are illustrated in Fig. 5.

All three current waveforms qualitatively resemble the experimental ones. The absence of the K^+ current eliminates the late outward currents in the intermediate and terminal waveforms. As a by-product, the second peak of inward current in the pre-terminal is lost because the Na^+ channels inactivate before a significant repolarization takes place. The depolarizations are large and long-lasting all over the nerve ending. The corresponding components of the total current are shown in Fig. 6.

The effect of local application of TTX cannot be reproduced

Brigant and Mallart (1982) showed that local ionophoretic application of Tetrodotoxin at the pre-

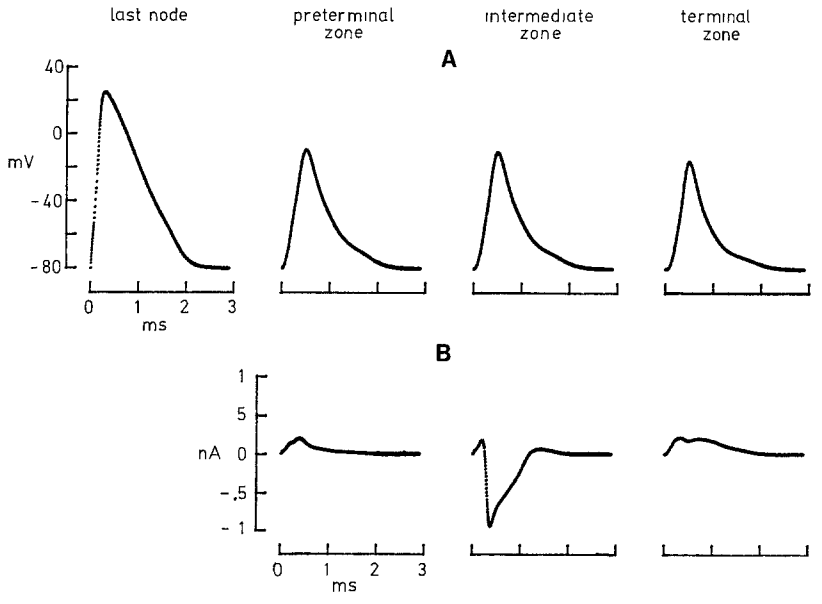

Fig. 7. Simulation of local block of Na^+ channels. Setting the Na^+ conductance to zero in the pre-terminal zone (Table 2, column 6) produces an outward current in the pre-terminal zone which is in disagreement with the experimental observations. Possible reasons for this discrepancy are discussed in the text

terminal led to the disappearance of the first peak of inward current. Assuming that TTX completely blocks the Na^+ conductance in this zone (i.e. $\bar{g}_{Na} = 0$), our model is not able to reproduce the experimental result. In fact, elimination of the Na^+ current, leaves only capacitive and leakage current in this zone. The net effect in our calculation is a modification from the double-peaked inward current to the small outward current shown in Fig. 7. However, a small and slow inward current can be produced by the model if $\bar{g}_{Na}$ is not set to zero but is reduced to one tenth of the value listed in Table 2 (column 4). In the light of our model, the residual inward current observed by Brigant and Mallart (1982) in the pre-terminal zone, after local application of TTX, might be due to an incomplete block of the Na^+ channels under the recording pipette.

Discussion

The purpose of this work was to verify whether a mathematical model including the main known morphological and electrophysiological features of a mammalian nervous termination was able to simulate the experimental observations. These are actually limited to the recording of membrane current with focal external electrodes and cannot give information about the amplitude of the currents because the resistance of the electrical seal between electrode and membrane is not known. However, the characteristic time course of the current at different positions along the terminal led Brigant and Mallart (1982) to suggest an uneven distribution of Na^+ and K^+ channels.

We have shown that it is possible to reproduce the essential features of the observed currents using the kinetic parameters measured in the node of Ranvier, provided the limiting conductances of Na^+ and K^+ are increased 5 and 20 times and Na^+ channels are present in the terminal branches. It is known that the density of Na^+ channels in the node of Ranvier is already high and this is explained by the fact that the node must be able to generate enough current to excite the next node some 1,000 μm away. However, the high insulation of the myelin sheath will greatly reduce current dispersion. The situation at the nerve terminal is much worse with regard to current dispersion because: *(i)* the myelin sheat is absent, *(ii)* several branches depart from the pre-terminal zone and *(iii)* the terminal branches do not possess (or possess in a much lower amount) Na^+ channels. Therefore a 5-fold increase in $\bar{g}_{Na}$ in the preterminal membrane might be justified by this peculiar geometrical and electrical situation. The increase in $\bar{g}_K$ required by our model to reproduce the experimental data (20 times) is larger than the one for Na^+. Such an increase, apparently unfavourable for the spread of excitation in the terminal, may be justified by the presence of a calcium current which may otherwise become regenerative. This increase is necessary for our model to reproduce the characteristic shape of the current waveforms. Also the increase in $\bar{g}_K$ becomes of the same order as that for Na^+ if one takes as a reference the limiting conductance value for potassium given by Hille (1971) (i.e. $\bar{g}_K = 0.130$ μS).

Using a value of 8.6 pS for the conductance of a single Na^+ channel (Conti et al. 1980; Neumcke et al. 1981) and a membrane area of 63 μm^2 for the reference node, the density of Na^+ channels is about 900/μm^2. Using a value of 6 pS for the K^+ single channel conductance (Conti et al. 1975), the density of K^+ channels turns out to be 1,800/μm^2.

The 10-fold reduction in leakage in the intermediate and terminal regions may be better justified. In fact, the g_L of the node is some 100 times higher than in other excitable preparations (Adrian et al. 1970) and this appears to be due to the fact that it is the only repolarizing current. Where the membrane possesses K^+ channels the role of the leakage current in repolarization is of secondary importance and therefore g_L may be much lower than in the node of Ranvier.

Our work has the obvious limit of being based on parameter estimates belonging to different membrane zones of the axon and in some cases to other species. It is possible that the ionic channels in the nerve terminal membrane have kinetic properties different from the ones observed in the node.

Our results suggest, however, that all inferences about the various components of the total membrane current recorded with focal electrodes must be drawn very carefully. Two examples may clarify this statement. The conclusion of Brigant and Mallart that no Na^+ channels are present in the terminal branches was based upon the absence of a negative component in the total current trace and to the lack of modifications of the current after TTX application. However, a small contribution of inward Na^+ current may be masked by the larger capacitive and ionic outward currents, as is shown in Fig. 4, and moreover this current could be TTX resistant. The second example concerns the late peak of inward current in the pre-terminal zone. The fact that the current is inwardly directed requires that its zero current potential has to be more positive than the membrane potential. The leakage current must have a zero current potential close to the resting potential, and therefore only Na^+ (with some contribution from the capacitive current) can be the carrier, being the only ion to have the required equilibrium potential.

References

Adrian RH, Chandler WK, Hodgkin AL (1970) Voltage clamp experiments in striated muscle fibres. J Physiol 208:607–644

Brigant JL, Mallart A (1982) Presynaptic currents in mouse motor endings. J Physiol 333:619–636

Chiu SY, Ritchie JM (1981) Evidence for the presence of potassium channels in the paranodal region of acutely demyelinated mammalian single nerve fibres. J Physiol 313:415–437

Chiu SY, Ritchie JM, Rogart RB, Stagg D (1979) A quantitative description of membrane currents in rabbit myelinated nerve. J Physiol 292:149–166

Conti F, DeFelice LJ, Wanke E (1975) Potassium and sodium ion current noise in the membrane of the squid giant axon. J Physiol 248:45–82

Conti F, Neumcke B, Nonner W, Stämpfli R (1980) Conductance fluctuations from the inactivation process of sodium channels in myelinated nerve fibres. J Physiol 308:217–239

Du Fort EC, Frankel SP (1953) Stability conditions in the numerical treatment of parabolic differential equations. Math Tab (Wash) 7:135–152

Fox L (1962) Numerical solution of ordinary and partial differential equations. Pergamon Press, Oxford

Hille B (1971) Voltage clamp studies on myelinated nerve fibers. In: Adelman WJ (ed) Biophysics and physiology of excitable membranes. Van Nostrand Reinhold, New York, pp 230–246

Katz B, Miledi R (1965) Propagation of electrical activity in motor nerve terminals. Proc R Soc B 161:453–482

Khodorov BI, Timin EN (1975) Nerve impulse propagation along nonuniform fibres. Prog Biophys Mol Biol 30: 145–184

Konishi T, Sears TA (1984) Electrical activity of mouse motor nerve terminals. Proc R Soc B 222:115–120

Llinas R, Steinberg IZ, Walton K (1981a) Presynaptic calcium currents in squid giant synapse. Biophys J 33:289–322

Llinas R, Steinberg IZ, Walton K (1981b) Relationship between presynaptic calcium current and postsynaptic potential in squid giant synapse. Biophys J 33:323–352

Mallart A, Brigant J-L (1982) Electrical activity at motor nerve terminals of the mouse. J Physiol (Paris) 78:407–411

Moore JW, Ramon F, Joyner RW (1975) Axon voltage-clamp simulations I. Methods and tests. Biophys J 15:11–35

Neumcke B, Schwarz W, Stämpfli R (1981) Block of Na channels in the membrane of myelinated nerve by benzocaine. Pflügers Arch 390:230–236

Parnas I, Segev I (1979) A mathematical model for conduction of action potentials along bifurcating axons. J Physiol 295:323–343

Quick DC, Kennedy WR, Donaldson L (1979) Dimensions of myelinated nerve fibers near the motor and sensory terminals in cat tenuissimus muscles. Neuroscience 4: 1089–1096